

AMP-Activated Protein Kinase Signaling Stimulates VEGF Expression and Angiogenesis in Skeletal Muscle

Noriyuki Ouchi, Rei Shibata, Kenneth Walsh

Abstract—AMP-activated protein kinase (AMPK) is regulated by various cellular stresses. Vascular endothelial growth factor (VEGF), a key regulator of angiogenesis, is also upregulated by several stress-inducible factors such as hypoxia and stimulation by cytokines and growth factors. Here, we investigated whether AMPK signaling in muscle has a role in regulating VEGF-mediated angiogenic processes. AICAR stimulated VEGF mRNA and protein levels in C2C12 myotube cultures. Transduction with dominant-negative AMPK abolished AICAR-induced VEGF expression at both steady state mRNA and protein levels. AICAR increased VEGF mRNA stability without affecting VEGF promoter activity. AICAR also stimulated p38 mitogen-activated protein kinase (p38 MAPK) phosphorylation. Activation of p38 MAPK was suppressed by transduction with dominant-negative AMPK, suggesting that AMPK is upstream of p38 MAPK. The p38 MAPK inhibitor SB203580 blocked AICAR-induced increase in VEGF mRNA and protein levels, indicating that AICAR-mediated VEGF induction is dependent on p38 MAPK signaling. AICAR treatment increased VEGF expression and accelerated angiogenic repair of ischemic hindlimbs in mice in an AMPK-dependent manner. These data indicate that AMPK-p38 MAPK signaling cascade can increase VEGF production in muscle and promote angiogenesis in response to ischemic injury. (*Circ Res.* 2005;96:838-846.)

Key Words: angiogenesis ■ AMP-activated protein kinase ■ vascular endothelial growth factor
■ p38 mitogen-activated protein kinase ■ skeletal muscle

AMP-activated protein kinase (AMPK) participates in the regulation of stress responses and metabolic homeostasis.¹ With regard to striated muscle, the AMPK signaling pathway is activated by hypoxia/ischemia,² vigorous exercise, and muscle contraction.^{2,3} Several studies show that AMPK activation by physiological and pharmacological stimuli, such as 5-aminoimidazole-4-carboxamide-1- β -D-ribofuranoside (AICAR), is associated with increased glucose uptake in muscle.^{1,4} AMPK stimulation with AICAR improves metabolic disorders associated with type 2 diabetes in animal models.^{1,5} Insulin also stimulates glucose uptake in muscle cells through activation of phosphatidylinositol-3 kinase (PI3-kinase)-dependent pathways,⁶ but the AMPK-mediated increase in glucose uptake is thought to be distinct from the PI3-kinase-dependent cascade.^{3,7} A recent report also showed that p38 mitogen-activated protein kinase (p38-MAPK) signaling participates in AICAR-stimulated glucose uptake in skeletal muscle.⁴

Vascular endothelial growth factor (VEGF) is an endothelial cell mitogen that has an essential role in both vasculogenesis and angiogenesis.⁸ VEGF expression patterns spatially and temporally correspond to the development of neovascularization under physiological and pathological conditions in vivo. VEGF expression is regulated by hypoxia,⁹

oxidative stress,¹⁰ and growth factors and cytokines.^{11,12} VEGF production is regulated at the levels of gene transcription,¹³ mRNA stability,⁹ and protein translation.¹⁴ VEGF is essential for the maintenance of the vascular network in skeletal muscle.¹⁵ Reduced expression of VEGF is associated with impaired ischemia-induced angiogenesis in the muscle tissues of diabetic or atherosclerotic animal models,^{16,17} and VEGF gene delivery has been shown to improve collateral vessel development in these models.¹⁶ It has also been shown that myogenic PI3-kinase/Akt signaling controls myofiber hypertrophy and VEGF expression downstream from insulin and IGF stimulation, leading to increase in blood vessel recruitment coupled to muscle growth.¹¹

Previously, we have demonstrated that AMPK signaling is required for angiogenic responses in endothelial cells under conditions of hypoxia in vitro.¹⁸ We have also shown that AMPK activator, adiponectin, promotes angiogenesis by activating AMPK signaling in endothelial cells and stimulates angiogenesis in response to ischemic stress in vivo.^{19,20} In the present study, we show for the first time that AMPK signaling in skeletal muscle modulates blood vessel growth through the production of an angiogenic growth factor. Using the pharmacological stimulator AICAR, we first examined the role of AMPK signaling in VEGF production in C2C12 myotubes.

Original received October 28, 2004; resubmission received February 14, 2005; revised resubmission received March 14, 2005; accepted March 15, 2005.

From the Molecular Cardiology/Whitaker Cardiovascular Institute, Boston University School of Medicine, Boston, Mass.

Correspondence to Kenneth Walsh, PhD, Molecular Cardiology/Whitaker Cardiovascular Institute, Boston University School of Medicine, 715 Albany St, W611, Boston, MA 02118. E-mail kxwalsh@bu.edu

© 2005 American Heart Association, Inc.

Circulation Research is available at <http://www.circresaha.org>

DOI: 10.1161/01.RES.0000163633.10240.3b

We also tested the effect of AICAR on blood vessel growth *in vivo* using a hindlimb model of ischemia-induced angiogenesis in mice. Our observations indicate that AICAR enhances VEGF expression via activation of an AMPK-p38 MAPK-dependent pathway in skeletal muscle, leading to the promotion of angiogenesis.

Materials and Methods

Materials

Phospho-AMPK (Thr172), pan- α -AMPK, phospho-p38 (Thr180/Tyr182), and p38 antibodies were from Cell Signaling Technology. Phospho-ACC (Ser79), ACC, and c-Myc tag antibody were from Upstate Biotechnology. VEGF antibody was from Santa Cruz Biotechnology. Tubulin antibody was from Oncogene. GAPDH antibody was from Biogenesis Inc. AICAR was from Toronto Research Chemicals Inc. Human insulin and 5-Iodotubercidin was from Sigma. LY294002, U0126, and SB203580 were from Calbiochem.

Cell Culture, Adenoviral Infection, and Western Blot Analysis

C2C12 mouse myoblasts (American Type Culture Collection) were cultured as described elsewhere.¹¹ Cells were maintained in growth medium (DMEM supplemented with 20% FBS). To induce differentiation, cells were shifted to differentiation medium (DMEM supplemented with 2% heat-inactivated horse serum) for 4 days. After differentiation, experiments were performed by the addition of the indicated amount of AICAR, insulin, or vehicle for the indicated lengths of time. In some experiments, C2C12 myocytes were pretreated with LY294002 (20 μ mol/L), 5-iodotubercidin (0.2 μ mol/L), U0126 (10 μ mol/L), SB203580 (10 μ mol/L), or vehicle for 1 hour before stimulation with AICAR or insulin. In some experiments, C2C12 myocytes were infected with adenoviral constructs encoding dominant-negative AMPK α 2^{18,19} or β -galactosidase (Adeno- β gal) at a multiplicity of infection (MOI) of 250 for 16 hours. Under these conditions, the transfection efficiency was greater than 90%. Hypoxia was generated by using a GasPak Plus system (Becton Dickinson). Cell or tissue samples were resolved by SDS-PAGE. The membranes were immunoblotted with the indicated antibodies followed by the secondary antibody conjugated with horseradish peroxidase (HRP). ECL Western Blotting Detection kit (Amersham Pharmacia Biotech) was used for detection. Mouse VEGF levels in cell culture media were determined with enzyme-linked immunosorbent assay (ELISA) kits (R&D Systems) used according to the manufacturer's protocol.

Determination of VEGF mRNA

Total RNA was prepared by Qiagen using protocols provided by the manufacturer. cDNA was produced using ThermoScript RT-PCR Systems (Invitrogen). Real-time PCR was performed on iCycler iQ Real-Time PCR Detection System (BIO-RAD) using SYBR Green I as a double-stranded DNA-specific dye according to manufacturer's instruction (Applied Biosystems) as described previously.²¹ Primers were as follows: 5'-CTGTAAACGATGAAGCCTGGAG-3' and 5'-TGGTGAGGTTTGATCCGCAT-3' for mouse VEGF; 5'-GATCATTGACCTGTCTCTGGACA-3' and 5'-GAGCCGCTCCATCAGCAG-3' for mouse tubulin; 5'-TCACCACCATGGAGAAGGC-3' and 5'-GCTAAGCAGTTGGTGGTGCA-3' for mouse GAPDH. In mRNA stability experiments, cells were treated with actinomycin D (5 μ g/mL) for the indicated lengths of time. VEGF mRNA levels were quantified by real-time PCR.

DNA Transfection and Measurement of VEGF Promoter Activity

The VEGF promoter-reporter constructs used in transient transfection assays contain sequences from the human VEGF promoter upstream (−2361 to +298) of the firefly luciferase gene.¹¹ Transient transfection was performed with Lipofectamine 2000 reagent (In-

vitrogen) by using protocols provided by the manufacturer. C2C12 cells were cotransfected with a VEGF promoter-reporter construct and a Renilla luciferase control plasmid (pRL-SV40, Promega) to normalize for transfection efficiency. At approximately 70% confluence, the medium was changed to differentiation medium. After differentiation, myotubes were incubated with AICAR, insulin, or vehicle. Cells were lysed and analyzed by using dual luciferase assay kit (Promega).

Mouse Model of Angiogenesis

Wild-type male mice in a C57/BL6 background were obtained from the Jackson Laboratory (Bar Harbor, Me) and used for this study. Study protocols were approved by the Institutional Animal Care and Use Committee in Boston University. Mice, at the age of 10 weeks, were subjected to unilateral hindlimb surgery under anesthesia with sodium pentobarbital (50 mg/kg intraperitoneally). In this model, the entire left femoral artery and vein were excised surgically.²⁰ AICAR (300 mg/kg per day) dissolved in 0.9% NaCl or vehicle (0.9% NaCl) was intraperitoneally injected 1 day before the operation and daily until euthanasia.⁵ Hindlimb blood flow was measured using a laser Doppler blood flow (LDBF) analyzer (Moor LDI; Moor Instruments). Immediately before surgery and on postoperative days 3, 7, 14, and 28, LDBF analysis was performed on legs and feet. Blood flow was displayed as changes in the laser frequency using different color pixels. To avoid data variations due to ambient light and temperature, hindlimb blood flow was expressed as the ratio of left (ischemic) to right (nonischemic) LDBF.²⁰ For adenovirus experiments, 2×10^8 plaque-forming units (pfu) of Ad-dnAMPK or Ad- β gal were injected into five different sites of adductor muscle in the ischemic limb 3 days before the ischemic hindlimb as previously described.²⁰

Immunohistochemical Analysis

Capillary density within thigh adductor muscle was quantified by histological analysis. Muscle samples were imbedded in OCT compound (Miles) and snap-frozen in liquid nitrogen. Tissue slices (5 μ m in thickness) were prepared and stained with anti-VEGF or anti-CD31 (PECAM-1; Becton Dickinson) antibodies. For capillary density analysis, 15 randomly chosen microscopic fields from 3 different sections in each tissue block were examined for the presence of capillary endothelial cells for each mouse specimen. Capillary density was expressed as the number of CD-31–positive features per high power field ($\times 400$) and the number of capillaries per muscle fiber.

Statistical Analysis

Data are presented as mean \pm SD. Differences were analyzed by Student unpaired *t* test. A level of *P* < 0.05 was accepted as statistically significant.

Results

AICAR Stimulates VEGF Expression in C2C12 Cells by Increasing mRNA Stability

Initially, we examined AICAR-mediated changes in the phosphorylation of AMPK (Thr172), and its downstream target ACC (Ser79) in differentiated C2C12 skeletal muscle cells by Western blot analysis. AICAR treatment induced the phosphorylation of AMPK and ACC in a time-dependent manner (Figure 1A). To examine whether AICAR regulates VEGF expression in C2C12 myocytes, VEGF protein levels in media were measured by ELISA. Treatment with AICAR at 0.5 or 2.0 mmol/L significantly increased the secretion of VEGF from C2C12 myotubes (Figure 1B). The effect of AICAR on VEGF secretion was comparable to that of insulin (10 nmol/L) (Figure 1B). AICAR treatment also stimulated VEGF steady-state mRNA levels quantified by real-time

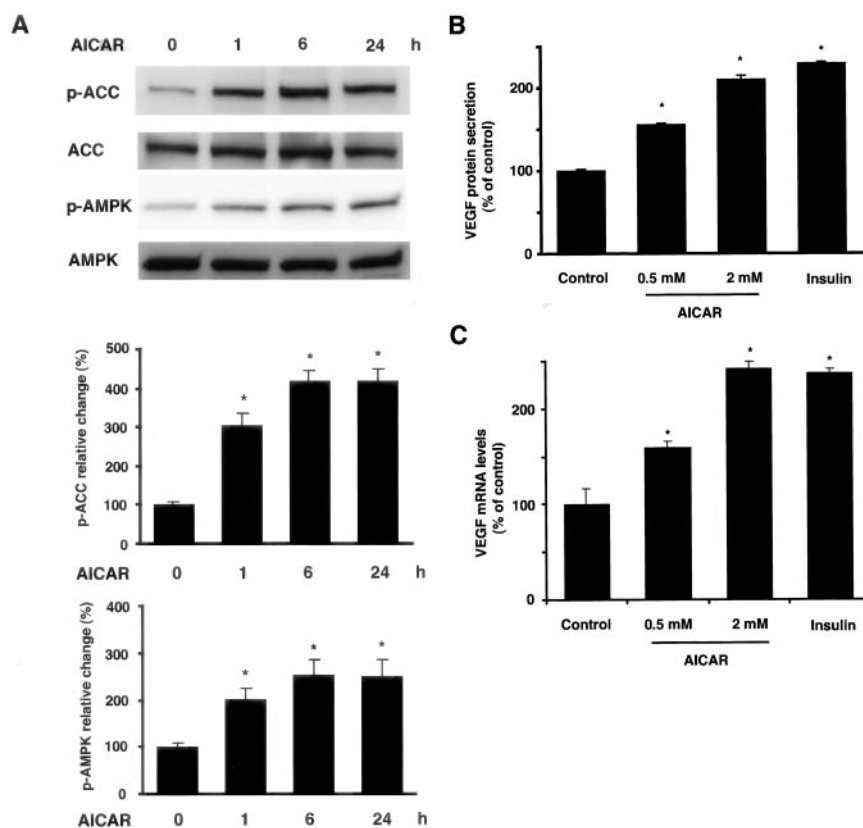


Figure 1. AICAR stimulates AMPK phosphorylation signaling and VEGF production in C2C12 myotubes. **A**, Time-dependent changes in the phosphorylation of AMPK (p-AMPK) and ACC (p-ACC) after AICAR treatment (2.0 mmol/L). Representative blots are shown. Relative phosphorylation levels of ACC and AMPK were quantified using NIH image program. Immunoblots were normalized to total loaded protein. * $P < 0.01$ vs control. **B**, Effect of AICAR on VEGF secretion from C2C12 myotubes. C2C12 cells were treated with AICAR (0.5 or 2.0 mmol/L), insulin (10 nmol/L) or vehicle (Control) for 24 hours. VEGF concentration was measured by ELISA. **C**, AICAR stimulates VEGF mRNA levels in C2C12 myotubes. C2C12 cells were treated with AICAR (0.5 or 2.0 mmol/L), insulin (10 nmol/L) or vehicle (Control) for 24 hours. VEGF mRNA levels were analyzed by quantitative real-time PCR method and expressed relative to levels of tubulin mRNA (arbitrary units). Results are expressed relative to control ($n = 3$). * $P < 0.01$ vs control.

PCR (Figure 1C). The stimulant effect of AICAR was similar to that of insulin (Figure 1C).

AICAR induces the accumulation of 5-aminoimidazole-4-carboxamide ribonucleotide (ZMP), which mimics AMP and activates AMPK signaling. 5-iodotubercidin, an inhibitor of adenosine kinase, blocks the formation of ZMP from AICAR and acts as an inhibitor of AICAR.²² Pretreatment with 5-iodotubercidin completely suppressed AICAR-induced VEGF mRNA and protein levels in C2C12 cells (Figure 2A and 2B). In contrast, 5-iodotubercidin did not change insulin-induced VEGF expression at both mRNA and protein levels (Figure 2A and 2B). Insulin increases VEGF expression via activation of the PI-3 kinase-dependent pathway,^{11,23} and the PI3-kinase inhibitor LY294002 significantly suppressed insulin induction of VEGF mRNA and protein levels (Figure 2A and 2B). However, LY294002 had no effect on AICAR-induced VEGF expression at mRNA or protein levels (Figure 2A and 2B). To examine the relative contribution of AMPK activation to the regulation of AICAR-stimulated VEGF expression, C2C12 myotubes were transduced with an adenoviral vector expressing a c-Myc-tagged dominant-negative mutant of AMPK (Ad-dnAMPK). Transduction with Ad-dnAMPK suppressed AICAR-induced ACC phosphorylation (Figure 2C). Transduction with Ad-dnAMPK also blocked AICAR-induced VEGF expression at mRNA and protein levels without affecting basal VEGF levels (Figure 2D and 2E). In contrast, transduction with Ad-dnAMPK had no effect on insulin-induced VEGF mRNA expression (data not shown). Collectively, these data suggest that AMPK is required for AICAR-mediated VEGF expression in C2C12

myotubes, and that VEGF induction by this mechanism is independent of PI3-kinase-dependent insulin signaling.

To test whether AICAR modulates VEGF expression at the transcriptional level, VEGF promoter-luciferase construct was analyzed in transfection experiments. AICAR treatment had no effect on the activity of the 2.6-kbp VEGF promoter fragment (Figure 3A). In contrast, insulin enhanced VEGF promoter activity, consistent with previous data.¹¹ These data suggested that AICAR stimulated VEGF expression in C2C12 cells at a posttranscriptional level. To test this possibility, VEGF mRNA stability experiments were performed. The decay of VEGF mRNA in the presence of actinomycin D was analyzed by quantitative real-time PCR. VEGF mRNA levels rapidly decreased in the absence of AICAR (Figure 3B). AICAR treatment led to a significant increase in VEGF mRNA stability in C2C12 myotubes, suggesting that AICAR-stimulated VEGF expression is due, at least in part, to increase in mRNA stabilization. In contrast, insulin had no effect on VEGF mRNA stability.

To investigate whether AICAR potentiates VEGF expression by hypoxia, C2C12 cells were incubated under hypoxic conditions in the presence or absence of AICAR. Hypoxia stimulated VEGF steady-state mRNA and protein levels in C2C12 cells (Figure 4A and B). AICAR treatment markedly enhanced VEGF expression at mRNA and protein levels in hypoxic cultures. Hypoxia slightly, but significantly, increased VEGF mRNA stability in C2C12 myotubes, whereas AICAR dramatically enhanced VEGF mRNA stability in the hypoxic cultures (Figure 4C). The HuR protein binds to the 3'-untranslated region of VEGF mRNA and promotes its

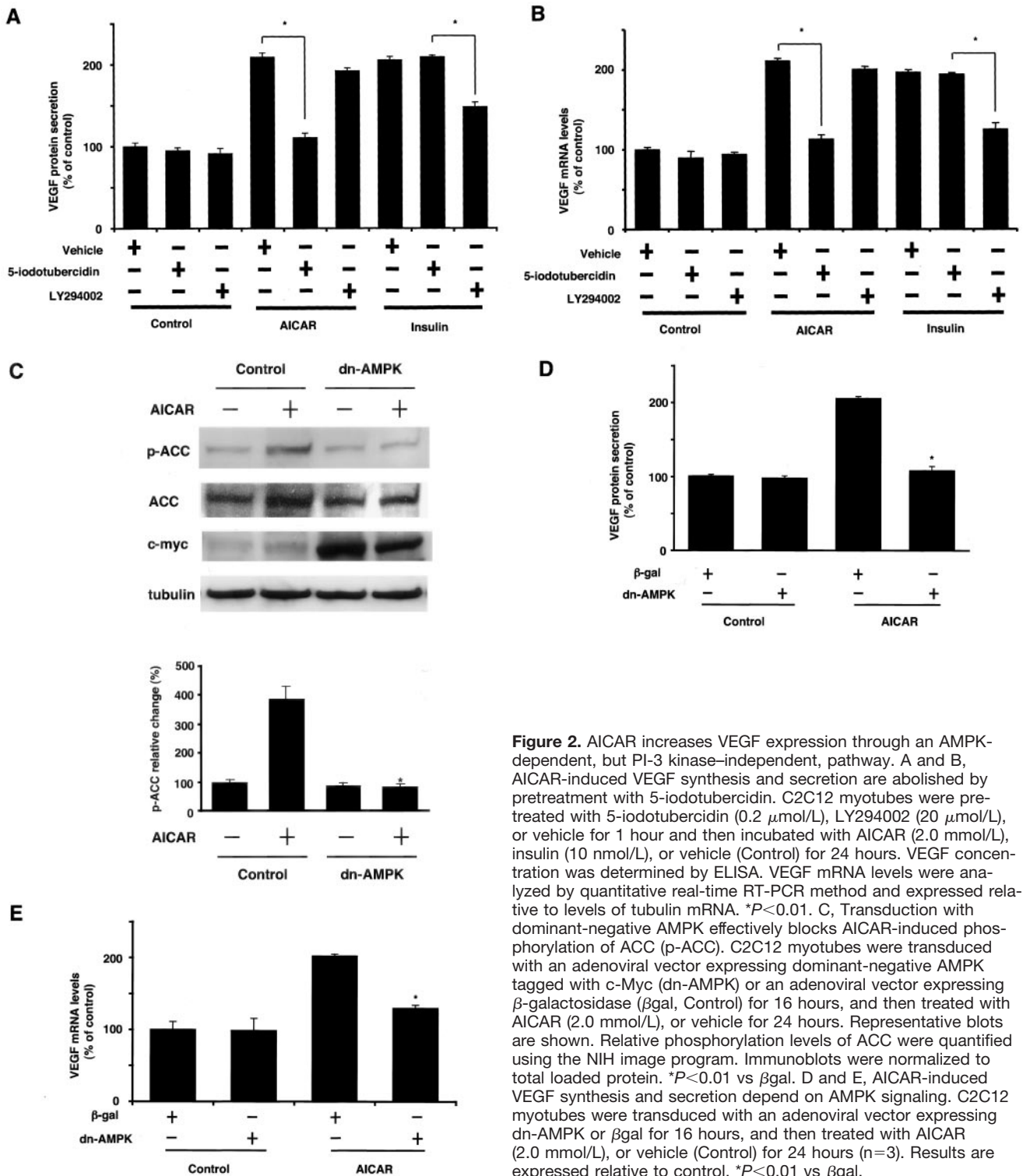


Figure 2. AICAR increases VEGF expression through an AMPK-dependent, but PI-3 kinase-independent, pathway. A and B, AICAR-induced VEGF synthesis and secretion are abolished by pretreatment with 5-iodotubercidin. C2C12 myotubes were pretreated with 5-iodotubercidin (0.2 μ mol/L), LY294002 (20 μ mol/L), or vehicle for 1 hour and then incubated with AICAR (2.0 mmol/L), insulin (10 nmol/L), or vehicle (Control) for 24 hours. VEGF concentration was determined by ELISA. VEGF mRNA levels were analyzed by quantitative real-time RT-PCR method and expressed relative to levels of tubulin mRNA. $*P < 0.01$. C, Transduction with dominant-negative AMPK effectively blocks AICAR-induced phosphorylation of ACC (p-ACC). C2C12 myotubes were transduced with an adenoviral vector expressing dominant-negative AMPK tagged with c-Myc (dn-AMPK) or an adenoviral vector expressing β -galactosidase (β gal, Control) for 16 hours, and then treated with AICAR (2.0 mmol/L), or vehicle for 24 hours. Representative blots are shown. Relative phosphorylation levels of ACC were quantified using the NIH image program. Immunoblots were normalized to total loaded protein. $*P < 0.01$ vs β gal. D and E, AICAR-induced VEGF synthesis and secretion depend on AMPK signaling. C2C12 myotubes were transduced with an adenoviral vector expressing dn-AMPK or β gal for 16 hours, and then treated with AICAR (2.0 mmol/L), or vehicle (Control) for 24 hours ($n = 3$). Results are expressed relative to control. $*P < 0.01$ vs β gal.

stability under conditions of hypoxia.²⁴ It is reported that AMPK activation inhibits the translocation of HuR from the nucleus to the cytoplasm and leads to the decrease in stability of target mRNAs including cyclin A, cyclin B1, and p21 in human colorectal carcinoma RKO cells.²⁵ However, AICAR treatment did not affect mRNA levels of cyclin A, cyclin B1, and p21 in C2C12 myotubes (N. Ouchi, unpublished results,

2005), suggesting that the stabilization of VEGF mRNA by AMPK activation is independent of HuR.

AICAR Increased VEGF mRNA Stability Through p38 MAPK Activation

The stress-activated protein kinase p38 MAPK is involved in mRNA stabilization of several genes including VEGF.^{26,27}

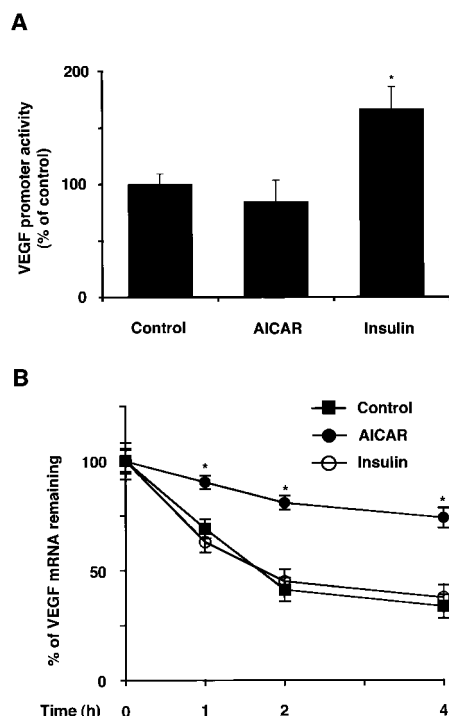


Figure 3. AICAR increases VEGF mRNA stability in C2C12 myotubes. **A**, Effect of AICAR on VEGF promoter activity. C2C12 cells were cotransfected with 2.6-kbp VEGF promoter constructs and SV40 promoter constructs. After myotube differentiation, cells were treated with AICAR (2.0 mmol/L), insulin (10 nmol/L) or vehicle (Control) for 16 hours ($n=3$). Cell extracts were analyzed by dual luciferase assay systems. Results are expressed relative to control. **B**, Effect of AICAR on VEGF mRNA stability. C2C12 myotubes were treated with AICAR (2.0 mmol/L), insulin (10 nmol/L), or vehicle (Control) for 3 hours before adding actinomycin D (5 μ g/mL) ($n=3$). mRNA levels were determined at 0, 1, 2, and 4 hours after adding actinomycin D. VEGF mRNA levels were quantified by real-time RT-PCR method and expressed relative to tubulin mRNA levels. Results are expressed relative to the values at time 0 hour. * $P<0.01$ vs control.

Therefore, we tested whether AICAR-induced VEGF expression was mediated by p38 MAPK. C2C12 cells were incubated with AICAR, and p38 MAPK phosphorylation at Thr180/Tyr182 was assessed by Western blot analyses. Treatment of C2C12 myotubes with AICAR enhanced the phosphorylation of p38 MAPK in a time-dependent manner (Figure 5A). In contrast, AICAR had no effect on ERK1/2 phosphorylation (data not shown). Transduction with AdnAMPK suppressed AICAR-induced p38 MAPK phosphorylation (Figure 5B), indicating that p38 MAPK is downstream of AMPK in C2C12 cells. To investigate whether p38 MAPK signal participates in AICAR-stimulated VEGF expression, C2C12 cells were incubated with p38 MAPK inhibitor, SB203580, in the absence or presence of AICAR. Treatment with SB203580 significantly suppressed AICAR-stimulated VEGF steady-state mRNA and protein levels (Figure 5C and 5D). The stimulation in VEGF mRNA levels was inhibited by 90%, 76%, and 42% using 10, 5, and 2 μ mol/L SB203580 (data not shown). The AICAR-stimulated increase in VEGF mRNA stability was also blocked by treatment with SB203580 (Figure 5E). However,

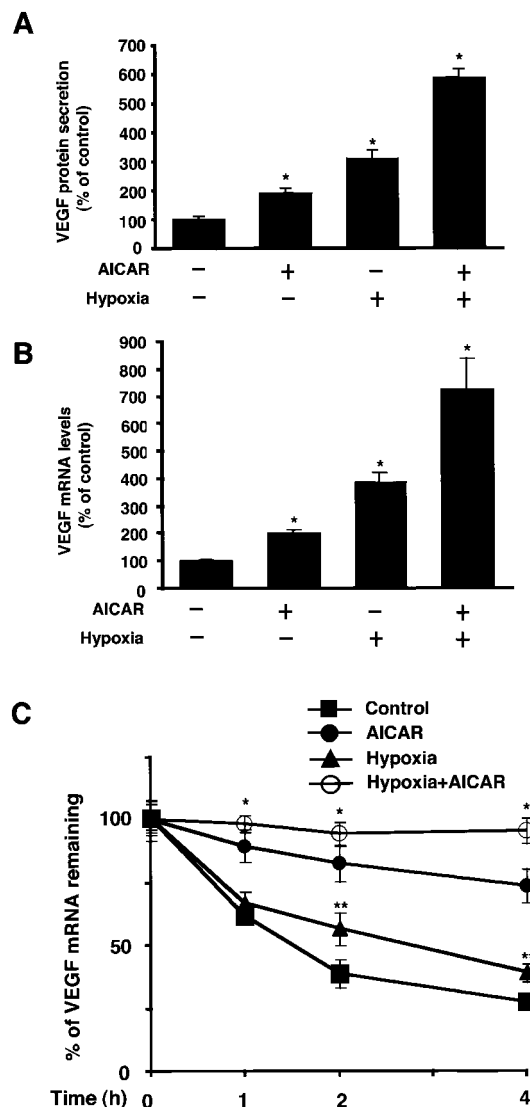


Figure 4. AICAR potentiates hypoxia-stimulated VEGF production in C2C12 myotubes. **A** and **B**, Effect of AICAR on hypoxia-induced VEGF synthesis and secretion in C2C12 myotubes. C2C12 cells were treated with AICAR (2.0 mmol/L) or vehicle under normoxic or hypoxic condition for 24 hours ($n=3$). **A**, VEGF protein concentration was determined by ELISA system. **B**, VEGF mRNA levels were analyzed by quantitative real-time PCR method and expressed relative to levels of tubulin mRNA. * $P<0.01$ vs vehicle under normoxic condition. **C**, Effect of AICAR on hypoxia-induced VEGF mRNA stability. C2C12 myotubes were treated with AICAR (2.0 mmol/L) or vehicle (Control) under normoxic or hypoxic condition for 3 hours before adding actinomycin D (5 μ g/mL) ($n=3$). mRNA levels were determined at 0, 1, 2, and 4 hours after adding actinomycin D. VEGF mRNA levels were quantified by QRT-PCR method and expressed relative to tubulin mRNA levels. Results are expressed relative to the values at time 0 hour. * $P<0.01$ vs without AICAR; ** $P<0.05$ vs control.

treatment with SB203580 did not affect the phosphorylation of AMPK and ACC (Figure 5F). The MEK inhibitor U0126 did not change AICAR-induced VEGF expression at both mRNA and protein levels (Figure 5C and 5D). These data indicate that p38 MAPK is critical for AICAR-induced VEGF expression and that p38 MAPK functions downstream from the AICAR-AMPK regulatory axis in myotubes.

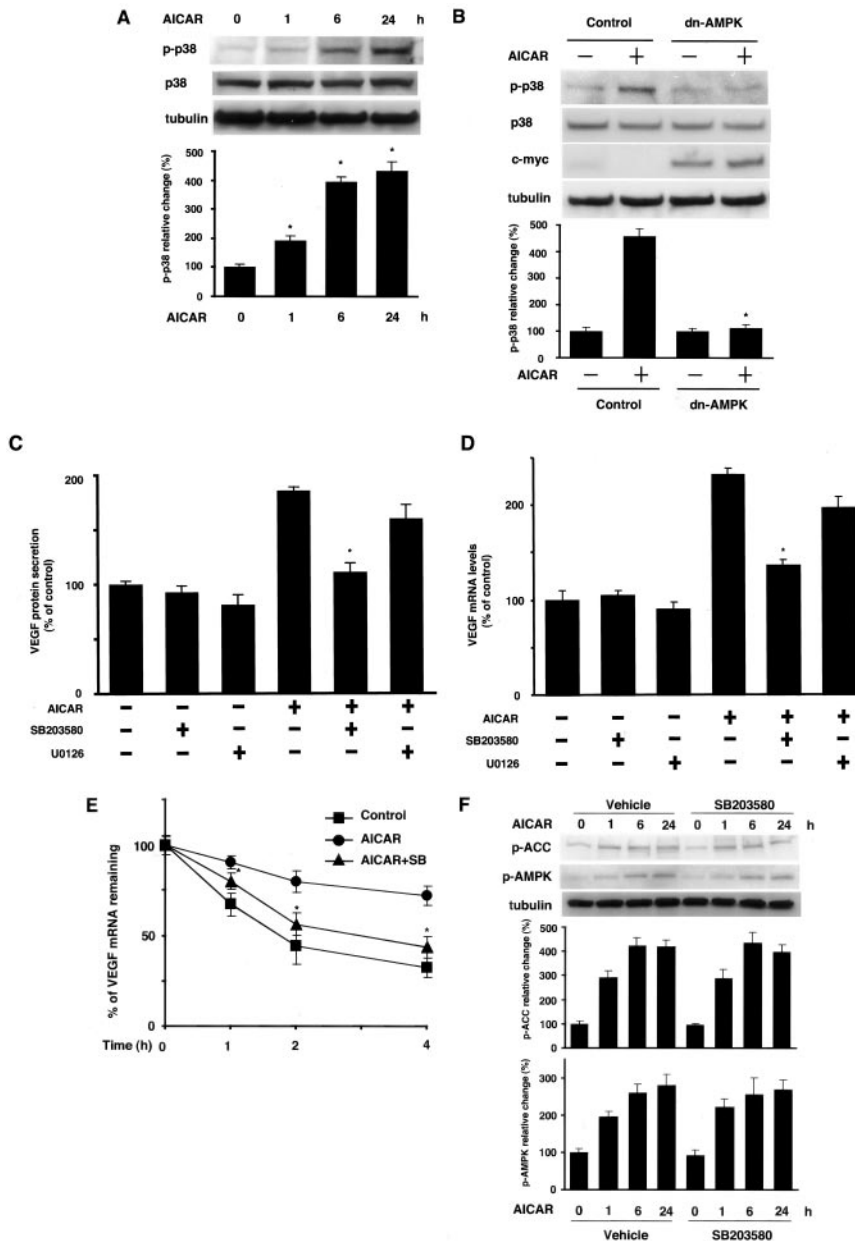


Figure 5. p38 MAPK signaling is involved in AICAR-induced VEGF production. **A**, Time-dependent changes in the phosphorylation of p38 MAPK (p-p38) after AICAR treatment (2.0 mmol/L). Representative blots are shown. Relative phosphorylation levels of p38 MAPK were quantified using the NIH image program. Immunoblots were normalized to total loaded protein. * $P < 0.01$ vs control. **B**, p38 MAPK is downstream of AMPK. C2C12 myotubes were transduced with an adenoviral vector expressing dn-AMPK or β gal (Control) for 16 hours, and then treated with AICAR (2.0 mmol/L), or vehicle for 24 hours. Relative phosphorylation levels of p38 MAPK were quantified using NIH image program. Immunoblots were normalized to total loaded protein. * $P < 0.01$ vs β gal. **C** and **D**, Effect of p38 MAPK inhibitor SB203580 on AICAR-stimulated VEGF synthesis and secretion. C2C12 myotubes were pretreated with SB203580 (10 μ mol/L), U0126 (10 μ mol/L), or vehicle for 1 hour and then incubated with AICAR (2.0 mmol/L) or vehicle for 24 hours ($n = 3$). VEGF concentration was measured by ELISA. VEGF mRNA levels were analyzed by quantitative real-time RT-PCR method and expressed relative to levels of tubulin mRNA. Results are expressed relative to control. **E**, Inhibitory effect of SB203580 on the increase in VEGF mRNA stability caused by AICAR. SB203580 (10 μ mol/L) or vehicle was pretreated for 1 hour, incubated with AICAR (2.0 mmol/L) or vehicle for 3 hours, and then stimulated with actinomycin D (5 μ g/mL) ($n = 3$). mRNA levels were determined at 0, 1, 2, and 4 hours after adding actinomycin D. VEGF mRNA levels were quantified by real-time RT-PCR method and expressed relative to tubulin mRNA levels. Results are expressed relative to the values at time 0 hour. * $P < 0.05$ vs AICAR treatment alone. **F**, Effect of SB203580 on AICAR-stimulated phosphorylation of ACC and AMPK. SB203580 (10 μ mol/L) or vehicle was pretreated for 1 hour and incubated with AICAR (2.0 mmol/L) or vehicle for the indicated length of time. Relative phosphorylation levels of ACC and AMPK were quantified using the NIH image program. Immunoblots were normalized to total loaded protein.

AICAR Promotes VEGF Synthesis and Angiogenesis in Ischemic Tissue In Vivo Through Activation of AMPK Signaling

To examine whether AMPK activation in muscle could promote angiogenesis in vivo, AICAR was intraperitoneally injected in mice that underwent unilateral femoral artery resection, a model of vascular insufficiency. AICAR treatment for 8 days stimulated the phosphorylation of AMPK and p38 MAPK in the ischemic muscle (Figure 6A). AICAR treatment also increased the VEGF mRNA and protein levels (Figure 6B). Immunohistochemical analysis indicated an elevated signal for VEGF protein in AICAR-injected mice compared with control mice that were treated with vehicle (Figure 6C). Importantly, AICAR-treated mice showed a significant increase in flow recovery at 7, 14, and 28 days after hindlimb surgery as determined by laser Doppler blood flow analysis (Figure 6D). To investigate the extent of

angiogenesis at the microcirculatory level, capillary density was measured in histological sections harvested from the ischemic tissues. Quantitative analysis revealed that the capillary density was significantly increased in AICAR-treated mice compared with control mice on postoperative day 7 (Figure 6E). No significant differences were observed in serum glucose levels between AICAR-injected and control mice (data not shown). Collectively, these results show that supplementation of AICAR can enhance VEGF production in ischemic muscle and promotes ischemia-induced angiogenesis.

To elucidate the role of AMPK signaling in AICAR-stimulated VEGF production and ischemia-induced angiogenesis in vivo, an adenoviral vector expressing a dominant-negative form of AMPK (Ad-dnAMPK) was injected intramuscularly into the adductor muscle of the ischemic limb. The intramuscular injection of Ad-dnAMPK significantly reduced both basal and AICAR-induced AMPK phos-

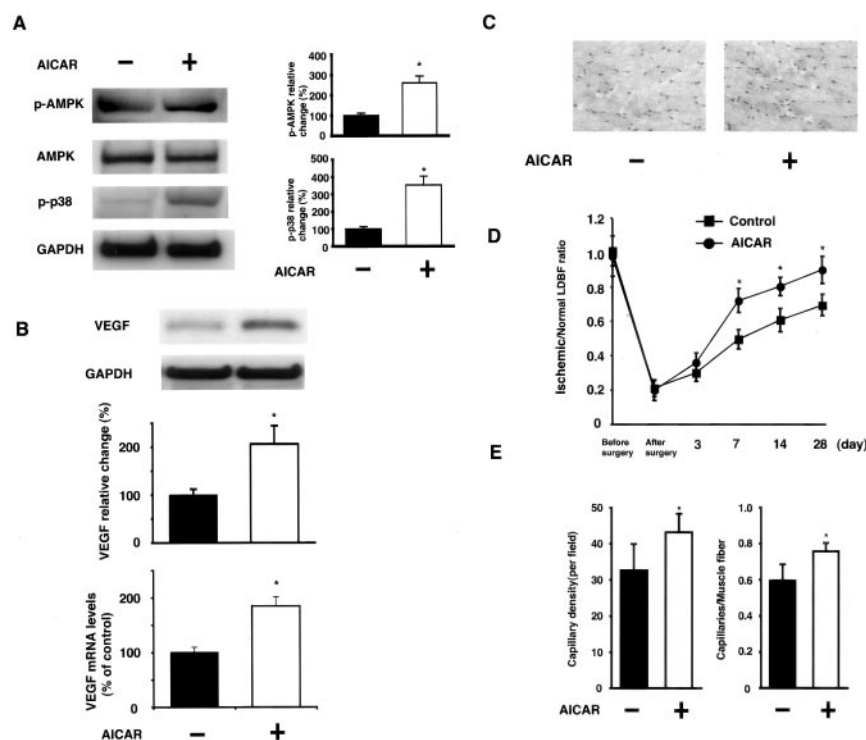


Figure 6. AICAR induces VEGF and promotes the reperfusion of ischemic limbs in mice in vivo. Hindlimb ischemic model was used to evaluate the effect of AICAR on angiogenesis in vivo. AICAR (300 mg/kg per day, $n=4$) dissolved in 0.9% NaCl or vehicle (Control, 0.9% NaCl, $n=4$) was injected intraperitoneally into mice. A, Effect of AICAR on the phosphorylation of AMPK (p-AMPK) and p38 MAPK (p-p38) in ischemic muscle of mice at 7 days after surgery. Representative phosphor-tyrosine blots are shown. Relative phosphorylation levels of ACC and AMPK were quantified using the NIH image program. Immunoblots were normalized to total loaded protein. $*P<0.01$ vs control. B, AICAR stimulated VEGF synthesis and protein levels in ischemic muscle tissues. On postoperative day 7, VEGF expression was determined by immunoblotting and real-time PCR analyses ($n=3$). Relative VEGF protein levels were quantified using the NIH image program. Immunoblots were normalized to total loaded protein. VEGF mRNA levels were expressed relative to levels of GAPDH mRNA. Results are expressed relative to control. $*P<0.01$ vs control. C, Immunostaining of ischemic tissues with anti-VEGF polyclonal antibody on postoperative day 7. D, Quantitative analysis of the

ischemic/nonischemic LDBF ratio in the AICAR-treated and vehicle-treated (Control) mice ($n=4$). $*P<0.01$ vs Control mice. E, Quantitative analysis of capillary density in the AICAR-treated and vehicle-treated (Control) mice ($n=4$). Immunostaining of ischemic tissues was performed with anti-CD31 monoclonal antibody. Capillary density was expressed as the number of capillaries per high power field ($\times 400$, left) and capillaries per muscle fiber (right). $*P<0.05$ vs Control mice.

phorylation in ischemic muscle (Figure 7A). Ad-dnAMPK also reduced AICAR-induced p38 MAPK phosphorylation without affecting basal p38 MAPK phosphorylation. In addition, the injection of Ad-dnAMPK suppressed AICAR-stimulated VEGF mRNA and protein levels (Figure 7B), and led to a significant reduction in the AICAR-mediated improvement in limb perfusion (Figure 7C). These data indicate that intramuscular AMPK signaling is crucial for basal and AICAR-induced VEGF expression and neovascularization after ischemic injury and that p38 MAPK is downstream from the AICAR-activated AMPK signaling in ischemic muscle.

Discussion

The present study demonstrates that the AMPK activator AICAR enhances VEGF mRNA stability and promotes VEGF protein secretion in skeletal muscle cells. AICAR supplementation also improved revascularization in ischemic limbs of mice. The ability of AICAR to stimulate VEGF production in muscle is likely to contribute to the stimulation of angiogenesis in this model. Additionally, AMPK activation will have direct proangiogenic effects on endothelial cells.^{18–20}

The stimulation of VEGF expression by AICAR is dependent on its ability to activate AMPK-p38 MAPK signaling. Transduction with dominant-negative AMPK $\alpha 2$ reduced AICAR-stimulated p38 MAPK phosphorylation and VEGF production in C2C12 myotubes, suggesting that p38 MAPK functions as downstream of AMPK under these conditions. In addition, the p38 MAPK inhibitor SB203580 blocked the

increase in VEGF mRNA stability and production caused by AICAR in C2C12 myotubes. It has been demonstrated that p38 MAPK signaling participates in the stabilization of VEGF mRNA,^{26,27} which is compatible with our data using AICAR. The PI3-kinase inhibitor LY294002 suppressed insulin-stimulated VEGF synthesis, in agreement with previous studies,^{11,23} but had no effect on the AICAR-induced VEGF expression in C2C12 myotubes. Taken together, AMPK-p38 MAPK signaling axis plays a crucial role in the regulation of VEGF production in muscle, and that this regulatory mechanism functions independently of PI3-kinase signaling (Figure 8).

In the present study, intramuscular injection of Ad-dnAMPK reduced both basal and AICAR-stimulated VEGF expression in ischemic muscle. In addition, Ad-dnAMPK reduced both basal and AICAR-stimulated AMPK phosphorylation in ischemic muscle, although Ad-dnAMPK reduced only AICAR-stimulated p38 MAPK phosphorylation without affecting basal p38 MAPK phosphorylation. Recently, it has been reported that AMPK is critical for HIF-1 transcriptional activity in hypoxic DU145 prostate cancer cells.²⁸ Although HIF-1 is a key transcriptional regulator of the VEGF gene,¹³ AICAR does not activate HIF-1 under normoxic conditions²⁸ (N. Ouchi, unpublished results, 2005). Taken together, it appears that the predominant effect of AMPK signaling on VEGF expression is the stabilization of the mRNA, whereas hypoxia and insulin stimulate VEGF expression by activation of transcription via different mechanisms.¹¹

It has been controversial whether p38 MAPK and p38 inhibitors act downstream or upstream of AMPK. Previous

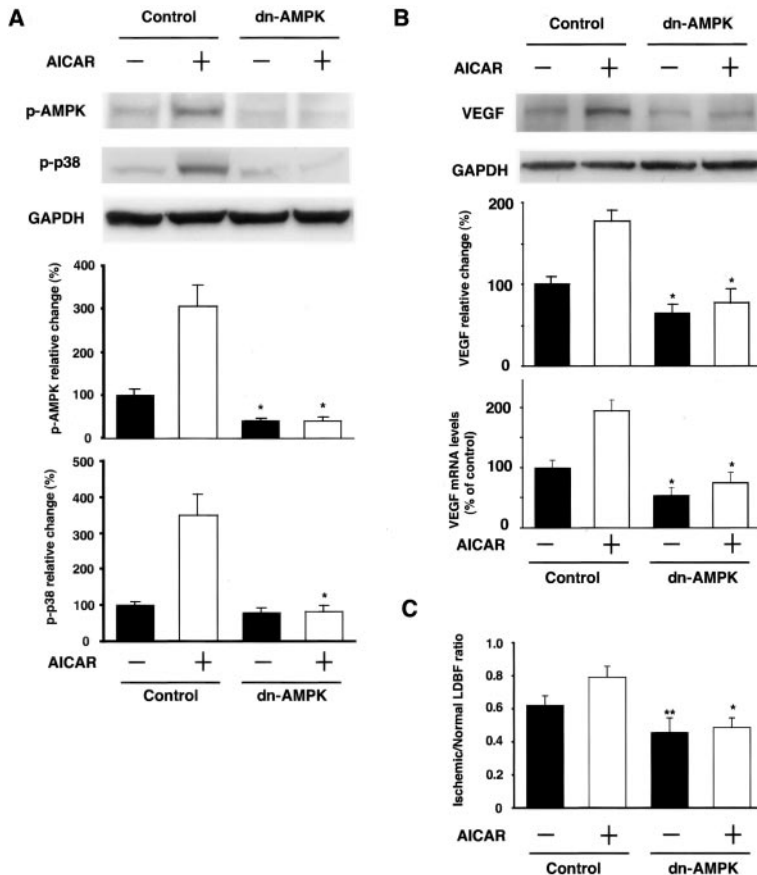


Figure 7. Contribution of AMPK signaling to AICAR-induced VEGF production and angiogenesis in ischemic hind limbs. Ad-dnAMPK (n=4) or Ad-βgal (Control, n=4) was injected into 5 sites in adductor muscle (2×10^8 pfu each), 3 days before ischemic surgery. AICAR or vehicle was injected intraperitoneally into mice. A, Effect of AMPK signaling on basal and AICAR-stimulated phosphorylation of AMPK (p-AMPK) and p38 MAPK (p-p38) in ischemic muscle of mice at 7 days after surgery. Representative blots are shown. Relative phosphorylation levels of ACC and AMPK were quantified using the NIH image program. Immunoblots were normalized to total loaded protein. * $P < 0.01$ vs control. B, Ad-dnAMPK suppresses basal and AICAR-stimulated VEGF synthesis and protein levels in ischemic muscle tissues. On postoperative day 7, VEGF expression was determined by immunoblotting and real-time PCR analyses. Relative VEGF protein levels were quantified using the NIH image program. Immunoblots were normalized to total loaded protein. VEGF mRNA levels were expressed relative to levels of GAPDH mRNA. Results are expressed relative to control. * $P < 0.01$ vs control. C, Quantitative analysis of ischemic/nonischemic LDBF ratio in mice hindlimb blood perfusion in the presence of AICAR or vehicle along with intramuscular injection of Ad-dnAMPK or Ad-βgal (Control) at 14 days postsurgery. Results are shown as the mean \pm SD. * $P < 0.01$ vs control; ** $P < 0.05$ vs control.

work has shown that AICAR increases glucose transport in a liver-derived cell line²⁹ and rat skeletal muscle⁴ and mice jejunum³⁰ through the activation of p38 MAPK. In contrast, it has been reported that SB203580 inhibits AICAR-induced AMPK activity in H-2K^b cells,³¹ perhaps through its ability to inhibit nucleoside transport.³² However, in our study, it is shown that whereas SB203580 inhibits AICAR-mediated VEGF induction, it did not affect AICAR-induced AMPK or ACC phosphorylation (Figure 5F). Similarly, it has been shown that SB203580 does not affect AICAR-stimulated AMPK or ACC phosphorylation in mouse jejunum or rat

skeletal muscle.^{4,30} Therefore, we conclude that AICAR induces p38 MAPK phosphorylation in C2C12 myotubes through activation of AMPK signaling.

AMPK activation using AICAR improves the metabolic abnormalities that are found in diabetic mice and rats.^{1,5} Clinically, collateral vessel development is impaired in diabetic patients with myocardial and limb ischemia,³³ and angiogenic therapy using VEGF is currently being considered for this patient population.³⁴ Therefore, pharmacological activators of AMPK signaling could produce beneficial metabolic changes as well as improve perfusion in subjects with insulin-resistant syndromes. Furthermore, AMPK signaling is anti-apoptotic in a variety of cell types, including endothelial cells,^{18,35} and AMPK-mediated eNOS phosphorylation will promote endothelial cell function.² Thus, AMPK activating agents could be useful for treating numerous pathological features that are associated with the diabetic phenotype.

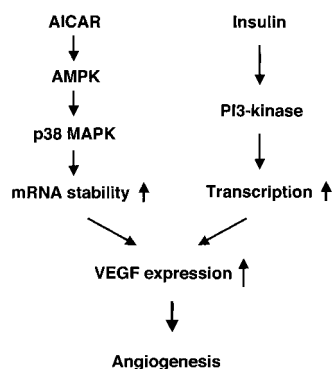
Acknowledgments

This work was supported by NIH grants HL77774, AR40197, AG15052, and AG17241 to K.W. We thank Ann Bialik for technical assistance.

References

- Hardie DG. Minireview: the AMP-activated protein kinase cascade: the key sensor of cellular energy status. *Endocrinology*. 2003;144: 5179–5183.
- Chen ZP, Mitchelhill KI, Michell BJ, Stapleton D, Rodriguez-Crespo I, Witters LA, Power DA, Ortiz de Montellano PR, Kemp BE. AMP-acti-

Figure 8. Proposed scheme for AMPK signaling pathway leading to VEGF induction. AICAR activates AMPK, which promotes p38 MAPK activation and increases VEGF mRNA stability. PI3-kinase participates in insulin-induced VEGF expression, but is independent of AICAR-AMPK-p38 stimulation of VEGF.



- vated protein kinase phosphorylation of endothelial NO synthase. *FEBS Lett.* 1999;443:285–289.
3. Hayashi T, Hirshman MF, Kurth EJ, Winder WW, Goodyear LJ. Evidence for 5' AMP-activated protein kinase mediation of the effect of muscle contraction on glucose transport. *Diabetes.* 1998;47:1369–1373.
 4. Lemieux K, Konrad D, Klip A, Marette A. The AMP-activated protein kinase activator AICAR does not induce GLUT4 translocation to transverse tubules but stimulates glucose uptake and p38 mitogen-activated protein kinases alpha and beta in skeletal muscle. *FASEB J.* 2003;17:1658–1665.
 5. Fiedler M, Zierath JR, Selen G, Wallberg-Henriksson H, Liang Y, Sakariassen KS. 5-aminoimidazole-4-carboxy-amide-1-beta-D-ribofuranoside treatment ameliorates hyperglycaemia and hyperinsulinaemia but not dyslipidaemia in KKAY-CETP mice. *Diabetologia.* 2001;44:2180–2186.
 6. Yeh JJ, Gulve EA, Rameh L, Birnbaum MJ. The effects of wortmannin on rat skeletal muscle. Dissociation of signaling pathways for insulin- and contraction-activated hexose transport. *J Biol Chem.* 1995;270:2107–2111.
 7. Fryer LG, Fougelle F, Barnes K, Baldwin SA, Woods A, Carling D. Characterization of the role of the AMP-activated protein kinase in the stimulation of glucose transport in skeletal muscle cells. *Biochem J.* 2002;363:167–174.
 8. Ferrara N. Molecular and biological properties of vascular endothelial growth factor. *J Mol Med.* 1999;77:527–543.
 9. Ikeda E, Achen MG, Breier G, Risau W. Hypoxia-induced transcriptional activation and increased mRNA stability of vascular endothelial growth factor in C6 glioma cells. *J Biol Chem.* 1995;270:19761–19766.
 10. Kuroki M, Voest EE, Amano S, Beerepoot LV, Takashima S, Tolentino M, Kim RY, Rohan RM, Colby KA, Yeo KT, Adamis AP. Reactive oxygen intermediates increase vascular endothelial growth factor expression in vitro and in vivo. *J Clin Invest.* 1996;98:1667–1675.
 11. Takahashi A, Kureishi Y, Yang J, Luo Z, Guo K, Mukhopadhyay D, Ivashchenko Y, Branellec D, Walsh K. Myogenic Akt signaling regulates blood vessel recruitment during myofiber growth. *Mol Cell Biol.* 2002;22:4803–4814.
 12. Wang D, Huang HJ, Kazlauskas A, Cavenee WK. Induction of vascular endothelial growth factor expression in endothelial cells by platelet-derived growth factor through the activation of phosphatidylinositol 3-kinase. *Cancer Res.* 1999;59:1464–1472.
 13. Semenza GL. HIF-1 and human disease: one highly involved factor. *Genes Dev.* 2000;14:1983–1991.
 14. Stein I, Itin A, Einat P, Skaliter R, Grossman Z, Keshet E. Translation of vascular endothelial growth factor mRNA by internal ribosome entry: implications for translation under hypoxia. *Mol Cell Biol.* 1998;18:3112–3119.
 15. Tang K, Breen EC, Gerber HP, Ferrara NM, Wagner PD. Capillary regression in vascular endothelial growth factor-deficient skeletal muscle. *Physiol Genomics.* 2004;18:63–69.
 16. Rivard A, Silver M, Chen D, Kearney M, Magner M, Annex B, Peters K, Isner JM. Rescue of diabetes-related impairment of angiogenesis by intramuscular gene therapy with adeno-VEGF. *Am J Pathol.* 1999;154:355–363.
 17. Couffignal T, Silver M, Kearney M, Sullivan A, Witzenbichler B, Magner M, Annex B, Peters K, Isner JM. Impaired collateral vessel development associated with reduced expression of vascular endothelial growth factor in ApoE^{-/-} mice. *Circulation.* 1999;99:3188–3198.
 18. Nagata D, Mogi M, Walsh K. AMP-activated protein kinase (AMPK) signaling in endothelial cells is essential for angiogenesis in response to hypoxic stress. *J Biol Chem.* 2003;278:31000–31006.
 19. Ouchi N, Kobayashi H, Kihara S, Kumada M, Sato K, Inoue T, Funahashi T, Walsh K. Adiponectin stimulates angiogenesis by promoting cross-talk between AMP-activated protein kinase and Akt signaling in endothelial cells. *J Biol Chem.* 2004;279:1304–1309.
 20. Shibata R, Ouchi N, Kihara S, Sato K, Funahashi T, Walsh K. Adiponectin stimulates angiogenesis in response to tissue ischemia through stimulation of amp-activated protein kinase signaling. *J Biol Chem.* 2004;279:28670–28674.
 21. Ouchi N, Kihara S, Funahashi T, Nakamura T, Nishida M, Kumada M, Okamoto Y, Ohashi K, Nagaretani H, Kishida K, Nishizawa H, Maeda N, Kobayashi H, Hiraoka H, Matsuzawa Y. Reciprocal association of C-reactive protein with adiponectin in blood stream and adipose tissue. *Circulation.* 2003;107:671–674.
 22. Musi N, Hayashi T, Fujii N, Hirshman MF, Witters LA, Goodyear LJ. AMP-activated protein kinase activity and glucose uptake in rat skeletal muscle. *Am J Physiol Endocrinol Metab.* 2001;280:E677–E684.
 23. Jiang ZY, He Z, King BL, Kuroki T, Opland DM, Suzuma K, Suzuma I, Ueki K, Kulkarni RN, Kahn CR, King GL. Characterization of multiple signaling pathways of insulin in the regulation of vascular endothelial growth factor expression in vascular cells and angiogenesis. *J Biol Chem.* 2003;278:31964–31971.
 24. Levy NS, Chung S, Furneaux H, Levy AP. Hypoxic stabilization of vascular endothelial growth factor mRNA by the RNA-binding protein HuR. *J Biol Chem.* 1998;273:6417–6423.
 25. Wang W, Fan J, Yang X, Furer-Galban S, Lopez de Silanes I, von Kobbe C, Guo J, Georas SN, Fougelle F, Hardie DG, Carling D, Gorospe M. AMP-activated kinase regulates cytoplasmic HuR. *Mol Cell Biol.* 2002;22:3425–3436.
 26. Winzen R, Kracht M, Ritter B, Wilhelm A, Chen CY, Shyu AB, Muller M, Gaestel M, Resch K, Holtmann H. The p38 MAP kinase pathway signals for cytokine-induced mRNA stabilization via MAP kinase-activated protein kinase 2 and an AU-rich region-targeted mechanism. *EMBO J.* 1999;18:4969–4980.
 27. Pages G, Berra E, Milanini J, Levy AP, Pouyssegur J. Stress-activated protein kinases (JNK and p38/HOG) are essential for vascular endothelial growth factor mRNA stability. *J Biol Chem.* 2000;275:26484–26491.
 28. Lee M, Hwang JT, Lee HJ, Jung SN, Kang I, Chi SG, Kim SS, Ha J. AMP-activated protein kinase activity is critical for hypoxia-inducible factor-1 transcriptional activity and its target gene expression under hypoxic conditions in DU145 cells. *J Biol Chem.* 2003;278:39653–39661.
 29. Xi X, Han J, Zhang JZ. Stimulation of glucose transport by AMP-activated protein kinase via activation of p38 mitogen-activated protein kinase. *J Biol Chem.* 2001;276:41029–41034.
 30. Walker J, Jijon HB, Diaz H, Salehi P, Churchill T, Madsen KL. 5-aminoimidazole-4-carboxamide riboside (AICAR) enhances GLUT2-dependent jejunal glucose transport: a possible role for AMPK. *Biochem J.* 2005;385:485–491.
 31. Fryer LG, Parbu-Patel A, Carling D. Protein kinase inhibitors block the stimulation of the AMP-activated protein kinase by 5-amino-4-imidazolecarboxamide riboside. *FEBS Lett.* 2002;531:189–192.
 32. Huang M, Wang Y, Collins M, Gu JJ, Mitchell BS, Graves LM. Inhibition of nucleoside transport by p38 MAPK inhibitors. *J Biol Chem.* 2002;277:28364–28367.
 33. Schaper W, Buschmann I. Collateral circulation and diabetes. *Circulation.* 1999;99:2224–2226.
 34. Syed IS, Sanborn TA, Rosengart TK. Therapeutic angiogenesis: a biologic bypass. *Cardiology.* 2004;101:131–143.
 35. Kobayashi H, Ouchi N, Kihara S, Walsh K, Kumada M, Abe Y, Funahashi T, Matsuzawa Y. Selective suppression of endothelial cell apoptosis by the high molecular weight form of adiponectin. *Circ Res.* 2004;94:e27–e31.